Terahertz time-domain spectroscopy of a simulated pore structure to probe particle size and porosity of porous rock*

Dong Chen(董 晨)[a)b)†], Bao Ri-Ma(宝日玛)[b)], Zhao Kun(赵 昆)[a)b)c)‡],
Xu Chang-Hong(许长虹)[b)], Jin Wu-Jun(金武军)[b)], and Zhong Shou-Xian(钟寿仙)[c)]

[a)] *State Key Laboratory of Petroleum Resources and Prospecting, China University of Petroleum, Beijing* 102249, *China*
[b)] *Beijing Key Laboratory of Optical Detection Technology for Oil and Gas, China University of Petroleum, Beijing* 102249, *China*
[c)] *Key Laboratory of Oil and Gas Terahertz Spectroscopy and Photoelectric Detection, China Petroleum and Chemical Industry Federation (CPCIF), Beijing* 100723, *China*

(Received 17 July 2014; revised manuscript received 1 September 2014; published online 10 October 2014)

The particle sizes and porosities of simulated pore structures are probed by terahertz time-domain spectroscopy. A double-peak time-domain spectrum phenomenon is observed when the terahertz (THz) pulses illuminated a pore and a particle. The amplitudes of the two peaks depend strongly and monotonically on the particle size and porosity. A model is used to study the phenomenon, and the computational results agreed with the experimental measurements. These measurements indicate the terahertz spectroscopic behaviors of pores and particles, suggesting that terahertz spectroscopy can be used as a noncontact probe of porosity.

Keywords: reservoir simulation, physical optics, terahertz spectroscopy, polymer

PACS: 78.20.Ci, 78.30.Jw, 78.47.jh **DOI:** 10.1088/1674-1056/23/12/127802

1. Introduction

The pore structure is highly significant in the evaluation of reservoir rock for oil and gas resources.[1] A real-time, noncontact, and nondestructive method of measuring the porosity of rock has real importance in the oil and gas industry to meet the need for a process analytical tool. The main methods of evaluating the pore structure include mercury intrusion, nitrogen absorption, nuclear magnetic resonance,[2] scanning electron microscopy (SEM), and computerized tomography.[3–5] The mercury intrusion and nitrogen absorption methods can yield information about porosity, particle size, pore volume, and other properties. SEM can provide two-dimensional information about the structure, although the necessary cutting and polishing operations may change the structure of the sample.[6] X-ray computed microtomography is used to visualize samples of different materials[7] with high-energy radiation and sophisticated equipment.

Terahertz (THz) radiation has low energy that is quickly detected, and can penetrate materials that are nonconductive and opaque at visible wavelengths. It also yields a higher spatial resolution than microwave radiation. THz radiation can be delivered from a handheld device that is compact, portable, and suitable for outdoor environments. THz time-domain spectroscopy (THz-TDS) is currently of great interest, for it has a variety of applications including industrial quality control, chemical and biological identification, pharmaceutical applications, security screening, and oil field applications.[8–20]

Particles of different sizes in the material forming a stack have various responses in the THz region.[21] Natural rock has a complex structure in which many factors affect the propagations of electromagnetic waves. In this paper, rocks are seen as a homogeneous mixture combined with pores, and the porosities and pore sizes of simulated samples are evaluated. We propose a new method of measuring rocks with different pore structures and suggest the applicability of THz-TDS technology to the evaluation of oil and gas reservoirs. We also introduce a phenomenon and explain it using a double-peak model, which also provides support for the development of oil–gas optics and offers a basis and direction for the analysis and characterization of pore structures with even smaller sizes using THz-TDS technology.

2. Experiment

In a typical conventional THz-TDS setup, a complete scan consists of a reference (air) scan and a sample (material) scan. A transmissive THz-TDS detection method was adopted.[21] The two types of simulated pore structures used in the experiments were made of a 0.63-mm-thick plastic sheet.[22–25] For Group 1, the plastic sheet was cut into squares with sizes of $L \times L$ (L = 3, 4, 5, 6, 8, and 10 mm) and glued onto a plastic board (25 mm × 25 mm) with epoxy as shown in Fig. 1(a). These samples simulated a pore structure with the same porosity (POR = 50%) and different particle sizes. In Group 2, the plastic sheet was cut into squares of the same size (L = 5 mm) as shown in Fig. 1(b), and used to simulate

*Project supported by the National Key Basic Research Program of China (Grant No. 2014CB744302), the Specially Funded Program on National Key Scientific Instruments and Equipment Development, China (Grant No. 2012YQ140005), and the Beijing Natural Science Foundation (Grant No. 4122064).

†Dong Chen and Bao Ri-Ma made equal contributions to this work.
‡Corresponding author. E-mail: zhk@cup.edu.cn

© 2014 Chinese Physical Society and IOP Publishing Ltd

pore structures with different porosities (POR = 0%, 31%, 49%, 61%, 69%, 75%, 80%, and 100%) and the same particle where the samples with POR = 0% and 100% were called the double-layer and single-layer samples, respectively. size,

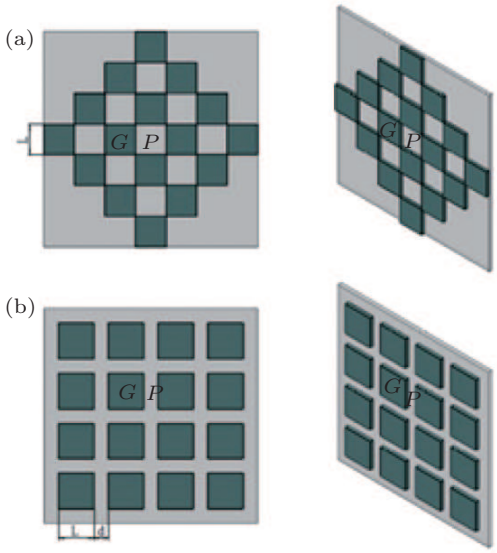


Fig. 1. (color online) Schematic drawings of samples, showing different particle sizes with (a) the same porosity of 50% (Group 1) and (b) different porosities with the same particle size of 5 mm (Group 2).

The center of the light spot of the THz-TDS equipment targets positions P and G (which represent pores and grains, respectively, as shown in Fig. 1) using a reference light (visible light) from a laser having the same optical axis as the THz beam. The samples were placed near but not on the focus, where the THz beam radius was about 4 mm–6 mm. A small amount of water content was maintained to reduce the attenuation of the THz energy.

3. Results and discussion

Figure 2 shows the time-domain waveforms of the THz electric field for the samples with different structures. An analysis of the time-domain spectra reveals three points: (i) the samples with different pore structures (particle size and porosity) can be distinguished by TDS; (ii) the spectral signal differs from the usual single-peak pulse signal, which is called double-peak phenomenon; (iii) the amplitudes of the two peaks depend strongly on L and the POR value. For example, as shown in Fig. 2(a), the amplitude of the first peak (V_{1P}^{1}) increases from 120 mV at $L = 3$ mm to 245 mV at $L = 10$ mm, while the second one (V_{1P}^{2}) decreases from 100 mV at $L = 3$ mm to 0 mV at $L = 10$ mm.

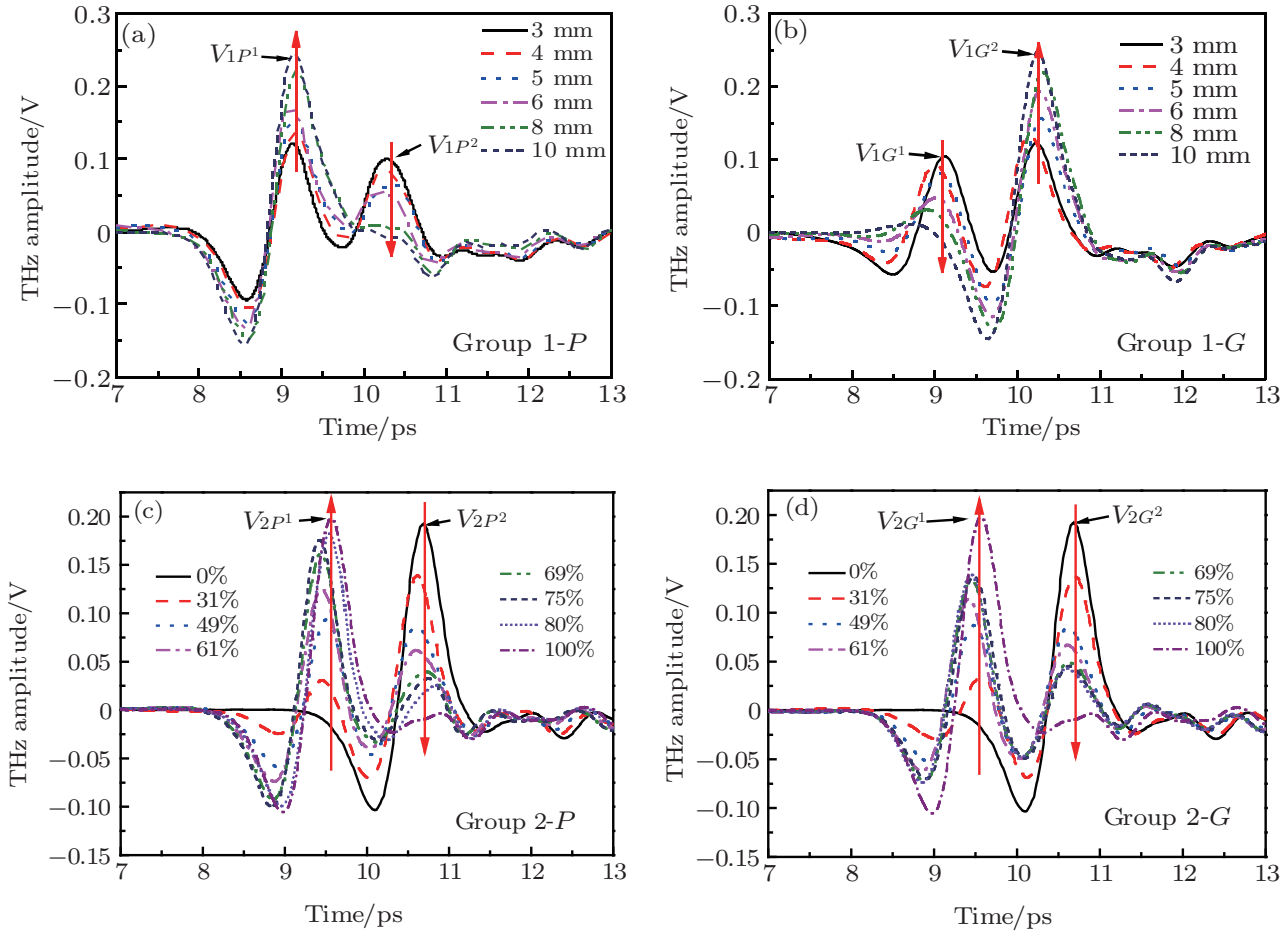


Fig. 2. (color online) THz time-domain spectra of Group 1 and Group 2 samples with the THz wave illuminating positions P and G: (a) Group 1-P and (b) Group 1-G for the pore structure with a POR of 50% and particle sizes ranging from 3 mm to 10 mm, (c) Group 2-P and (d) Group 2-G for the pore structure with a particle size of 5 mm and POR values ranging from 0% to 100%.

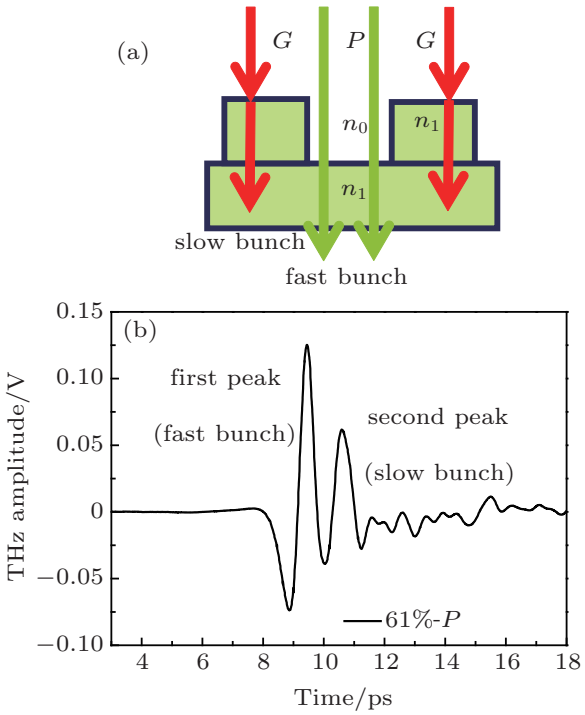


Fig. 3. (color online) (a) Schematic diagram of double-peak model and (b) the variations of THz signals of a fast bunch and a slow bunch with time.

Because $n_1 > n_0$, where n_0 and n_1 are the refractive indices of the reference and plastic sheet, respectively, and indicate the different transmission speeds of electromagnetic waves, the THz waves are divided into a fast bunch and a slow bunch when they pass through the sample as shown in Fig. 3. The fast bunch arrives at the detector first, and the peak signal is generated at the position of the single-layer plastic sheet, while the slow bunch arrives later and generates a peak signal at the position of the double-layer plastic sheet. The two waves are added and form an actual signal. Therefore, the following equation:

$$F(t) = f_1(t) + f_2(t), \tag{1}$$

can be used to explain this phenomenon, with the errors taken into consideration. In Eq. (1), $F(t)$ is the wave function of the sample, and $f_1(t)$ and $f_2(t)$ are the wave functions of the fast and slow waves, respectively. Equation (1) can be modified into

$$F(t) = \alpha_1\zeta_1 f(t+\Delta T_1) + \alpha_2\zeta_2 f(t+\Delta T_2), \tag{2}$$

where α_i is the attenuation coefficient and is equal to A_i/A_0, $f(t)$ is the wave function for the case without the sample, ΔT_i is the relative time delay, A_i is the peak amplitude, ζ_i is the coefficient that corrects for superposition and $i = 1$ or 2 denotes fast or slow waves, respectively. The correction coefficient is based on the ratio between the two peaks in the actual TDS and the first calculation of $F(t) = \alpha_1 f(t+\Delta T_1) + \alpha_2 f(t+\Delta T_2)$. Figures 4(a) and 4(b) show the THz-TDS signals for THz irradiation of position P in the samples with porosities of 31% and 75%, respectively. The results calculated using Eq. (2) are identical to the results of the actual signals, indicating the feasibility and reasonableness of the double-peak model. Table 1 shows the parameters needed in Eq. (2). Thus, the pore space and particle size of the sample, as well as their ratio (which is also called the porosity) can be calculated if an appropriate model is adopted.

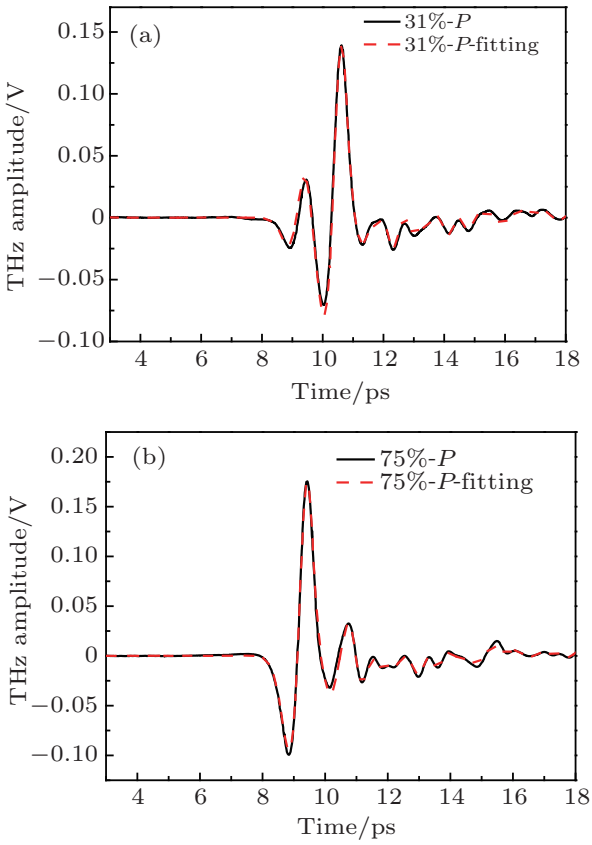


Fig. 4. (color online) Experimental (black) and calculated (red) results from the double-peak model with (a) 31% porosity and (b) 75% porosity

Table 1. Sample parameters needed in Eq. (2).

Sample	ΔT_1	α_1	ζ_1	ΔT_2	α_2	ζ_2
31%-*P*	0.96	0.14	1.33	2.14	0.65	1.00
75%-*P*	0.95	0.82	1.00	2.27	0.15	1.00

Figure 5 shows the variations of peak amplitudes of the THz signals with particle size for Groups 1-*P* and 1-*G*, and with porosity for 2-*P* and 2-*G*, respectively. By increasing the particle size and porosity, the peak signal amplitude changes monotonically. As shown in Fig. 5(a) for L ranging from 3 mm to 10 mm, V_{1P}^1 increases from 120 mV to 245 mV at a rate of 17.85 mV/mm. Correspondingly, V_{1P}^2 changes from 100 mV to 0 mV at a rate of −14.28 mV/mm. In contrast, when the THz wave illuminates position G, the first peak V_{1G}^1 decreases from 104 mV to 0 mV, and the second peak, V_{1G}^2, increases from 123 mV to 250 mV. On the other hand, as shown in Figs. 5(c) and 5(d), the first peaks, V_{2P}^1 and V_{2G}^1, increase from 0 mV to 182 mV and 140 mV as the porosity changes from 0% to 80%, and the second peaks, V_{2P}^2 and V_{2G}^2, decrease from 192 mV to 25 mV and 43 mV, respectively.

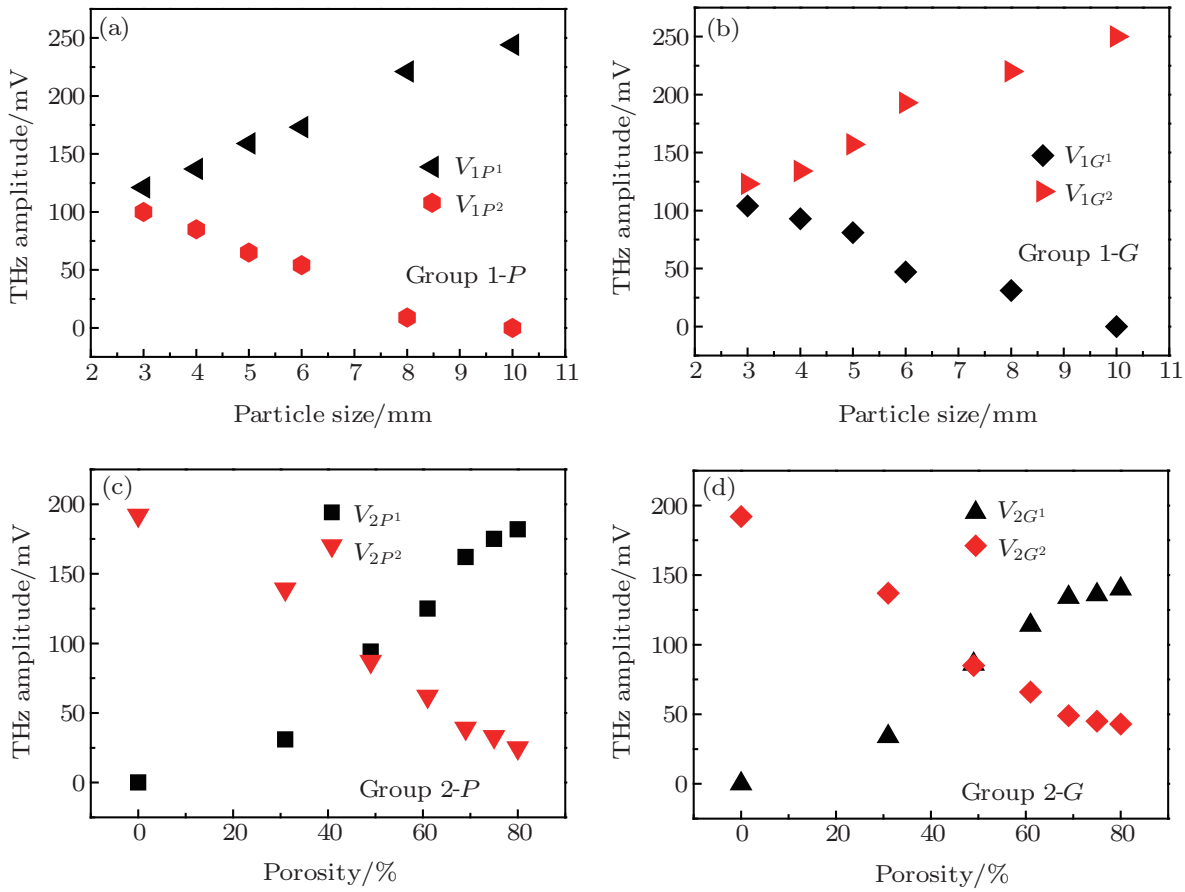


Fig. 5. (color online) Variations of THz peak amplitudes extracted from THz-TDS with particle size for Groups 1-*P* (a) and 1-*G* (b), and with porosity for Groups 2-*P* (c) and 2-*G* (d).

As we can see from the amplitude in Fig. 3, the THz-TDS technology can be used to distinguish diverse pore structures qualitatively. We can even expect to distinguish the pore structures semiquantitatively and quantitatively in the future. This research, as well as further analysis of the double-peak phenomenon, will be realized gradually in later experiments. Compared with THz imaging technology, the method in this paper is fast and easy to analyze. Compared with traditional focus-type THz-TDS, this method avoids errors generated by evaluating a single point. Encouragingly, our experimental results would facilitate the application of THz-TDS technology to the evaluation of the oil and gas reservoirs associated with unconventional oil and gas resources.

4. Summary and outlook

In this paper, we extend the investigation of the properties of different pore structures by taking into account their THz band response. THz spectra show that different particle sizes and porosities can be obviously distinguished by the peak values in a double-peak phenomenon. Petroleum is one of the most important nonrenewable energy resources in the world. A deeper understanding of the porosity of rock with respect to oil and gas generation would play a role in solving the current energy problem in the world. Being nondestructive and contactless, THz technology shows great promise for improving porosity analysis; it can be established as a key tool in petroleum exploration and thus positively affect the oil and gas industry.

References

[1] Javadpour F, Fisher D and Unsworth M 2007 *J. Canadian Petro. Tech.* **46** 55

[2] Westphal H, Surholt I, Kiesl C, Thern H F, and Kruspe T 2005 *Pure Appl. Geophys* **162** 549

[3] Biswal B, Held R J, Khanna V, Wang J and Hilfer R 2009 *Phys. Rev. E* **80** 041301

[4] Tariq F, Haswell R, Lee P D and McComb D W 2011 *Acta Mater.* **59** 2109

[5] Martinez-Angeles R and Perez-Rosales C 2000 *SPE International Petroleum Conference and Exhibition in Mexico*, February 1–3, 2000, Villahermosa, Mexico, 58990MS

[6] Lamea O, Belleta D, Michielb M D and Bouvard, D 2004 *Acta Mater.* **52** 977

[7] Bernard D, Gendron D, Heintz J M, Bord'ere S and Etourneau J 2005 *Acta Mater.* **53** 121

[8] Upadhya P C, Shena Y C, Daviesb A G and Linfield E H 2004 *Vib. Spectrosc.* **35** 139

[9] Nishizawaa J, Sasakia T, Sutoa K, Yamadab T, Tanabeb T, Tannoa T, Sawaic T and Miurac Y 2005 *Opt. Commun.* **244** 469

[10] Zhang X C, Hu B B, Darrow J T and Auston D H 1990 *Appl. Phys. Lett.* **56** 1011

[11] Heilweil E J, Maslar J E, Kimes W A, Bassim N D and Schenck P K 2009 *Opt. Lett.* **34** 1360

[12] Baxter J B and Glenn G W 2011 *Anal. Chem.* **83** 4342

[13] Globus T, Woolard D, Crowe T W, Khromova1 T, Gelmont B and Hesler J 2006 *J. Phys. D: Appl. Phys.* **39** 3405

[14] Scales A J and Batzle M 2006 *Appl. Phys. Lett.* **88** 062906

[15] Al-Douseri F M, Chen Y Q and Zhang X C 2006 *Int. J. Infr. Millim. Waves* **27** 481

[16] Ikeda T, Matsushita1 A, Tatsuno M, Minami Y, Yamaguchi M, Yamamoto K, Tani M and Hangyo M 2005 *Appl. Phys. Lett.* **87** 034105

[17] Leng W X, Ge L N, Xu S S, Zhan H L and Zhao K 2014 *Chin. Phys. B* **23** 107804

[18] Jin W J, Li T, Zhao K and Zhao H 2013 *Chin. Phys. B* **22** 118701

[19] Zhao H, Zhao K, Tian L, Zhao S Q, Zhou Q L, Shi YL, Zhao D M and Zhang C L 2012 *Sci. China: Series G* **55** 195

[20] Bao R M, Wu S X, Zhao K, Zheng L J and Xu C H 2013 *Sci. China: Series G* **56** 1603

[21] Yan H G, Li X S, Chandra B, Tulevski G, Wu Y, Freitag M. Zhu W J, Avouris P and Xia F 2012 *Nat. Nanotechnology* **7** 330

[22] Pastorelli G, Trafela T, Taday P F, Portieri A, Lowe D, Fukunaga K and Strlič M 2012 *Anal. Bioanal. Chem.* **403** 1405

[23] Kaushik M, Ng B W H, Fischer B M and Abbott D T 2012 *Appl. Phys. Lett.* **100** 011107

[24] Franz M, Fischer B M and Walther M 2008 *Appl. Phys. Lett.* **92** 0211072

[25] Nam K M, Zurk L M and Schecklman S 2012 *Prog. Electromagn. Res. B* **38** 205